Supplemental Materials

Molecular Biology of the Cell

Hayashi et al.

Supplementary Materials
Legends for Supplemental Figures S1-S5

Figure S1. Evaluation of the errors in the estimation of the fluctuation χ.

Panels (**A**) and (**B**) represent an example of anterograde and retrograde vesicles, respectively. The left panels show the comparison of the method to estimate the Gaussian distribution from the observed ΔX values. The thick curves represent the estimation from the histogram of ΔX, which can be biased by binning. The thin blue curves are based on the fitting of the cumulative Gaussian distribution. The thin red curves show the results by simply calculating the average and the variance of ΔX, which can be biased by the tails of the distribution. The right panels show 10 sample results of the bootstrapping confirmation for the errors in the estimation. These bootstrapping results gave an estimate for the errors in the estimation of the fluctuation χ as 10% CV, which is consistent with the expected errors from the accuracy of the position measurement (8 nm).

Figure S2. Analysis of the relaxation time.

(A) The relaxation time τ was estimated by fitting of the function $c(1-\exp(-\Delta t/\tau))$ to χ, where c is a constant. In this paper, the converged value of χ^* was calculated as χ at Δt=51 ms, noting that χ at Δt=51 ms is the same as c within the error of χ. **(B, C)** The fluctuation of the endosomes was analyzed in permeabilized and reactivated neurons, in which the ATP concentration was maintained at 125 μM and 12.5 μM. Both anterograde (B) and retrograde (C) endosomes showed slower relaxation when ATPase cycle was slowed down. The relative cycle time was calculated as $1+K_m/[ATP]$, where the Michaelis-Menten constant K_m was assumed to be 50 μM as an approximate value for both kinesin and dynein. The data are shown as box-and-whisker plots. 35 anterograde and 27 retrograde vesicles (from 29 and 24 cells) were analyzed for [ATP]=125 μM. 15 vesicles each (from 9 and 14 cells) for [ATP]=12.5μM.

Figure S3. Relation between velocity and χ^* for the kinesin-coated bead.

(A) An example of the trace of displacement $X(t)$ of the bead, carried by kinesin motors, obtained in the *in vitro* experiment using an optical tweezers instrument (the stiffness of the trap was 0.1 pN/nm). Here loads on the beads were applied by optical tweezers(F_{opt}) mimicking the high viscous effect acting on cargo vesicles in cells. Segments for the analysis in the graph indicated with red and green were determined by fitting the trajectory to the constant velocity movement. (inset) Analysis of fluctuation, calculated as $\Delta X=X(t+\Delta t)-X(t)$. **(B)** Distribution of ΔX at Δt=30 ms fitted by a Gaussian function. **(C)** Relaxation of χ. χ^* and τ denote the value of convergence and the time constant, respectively. **(D)** Linear relation between χ^* and v for the traces with the stall force <12 pN (closed squares (n=29)) and >12 pN (open squares (n=16)). The data points aligned linearly, supporting equation (9). The same proportional relation for the open and closed symbols indicates that the proportional coefficient ($k_{\mathrm{B}}T_{eff}/\Gamma$) was not sensitive to the number of motors attached to the beads.

Figure S4. Velocity distributions of endosomes.

Velocity distributions of endosomes for anterograde transport **(A)** and retrograde transport **(B)**. Only the segments of constant velocity movement with durations longer than 2 s were analyzed (e.g. rectangles depicted in Figure 3B). The mean velocities were 1.2 ± 0.7 μm/s (mean ± SD, n=145) for anterograde transport, and 1.3 ± 0.8 μm/s (n=163) for retrograde transport,

respectively. It should be noted that the velocities distributed more continuously without clear distinct peaks, which appears very differently from the distributions of χ^* (Figure 4A, 5A).

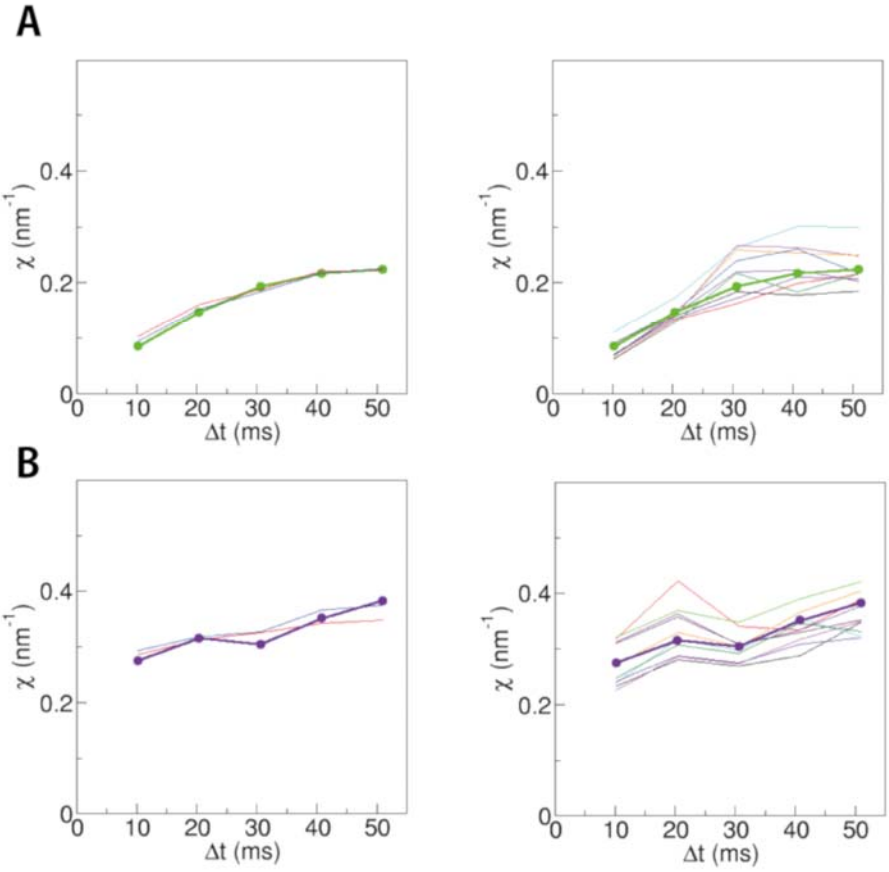

Fig S1. Hayashi et al.

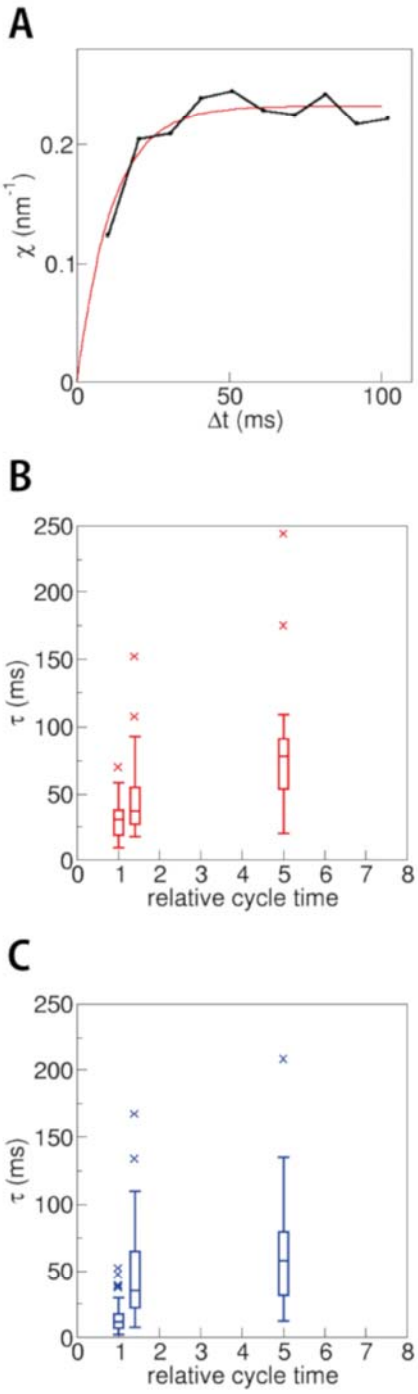

Fig S2. Hayashi et al.

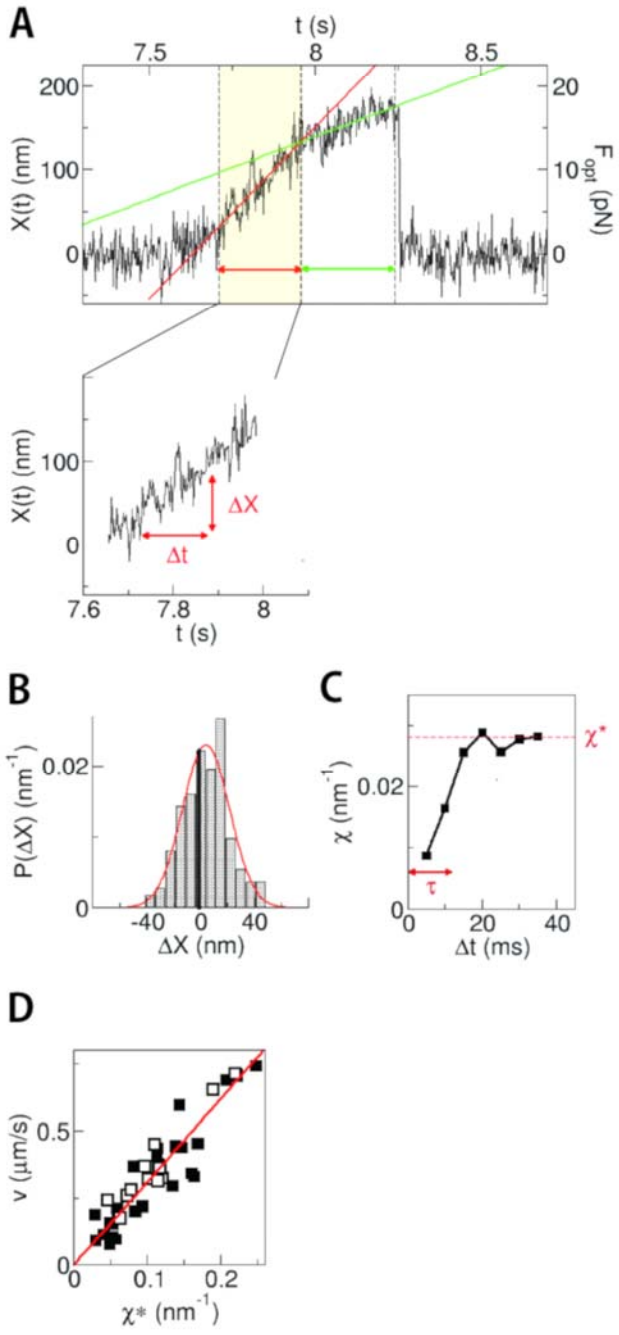

Fig S3. Hayashi et al.

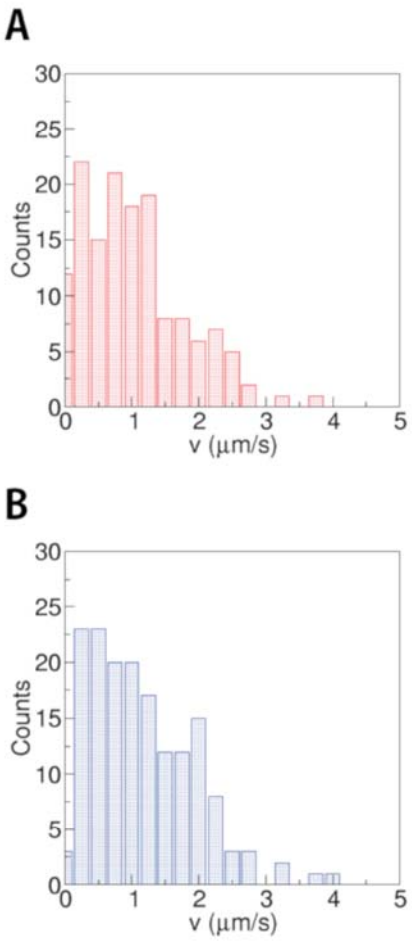

Fig S4. Hayashi et al.